Front. Earth Sci. 2018, 12(2): 361–372
https://doi.org/10.1007/s11707-017-0673-9

RESEARCH ARTICLE

Exploring the heavy air pollution in Beijing in the fourth quarter of 2015: assessment of environmental benefits for red alerts

Teng NIE[1], Lei NIE[1], Zhen ZHOU[1], Zhanshan WANG (✉)[2], Yifeng XUE (✉)[1], Jiajia GAO[3], Xiaoqing WU[1], Shoubin FAN[1], Linglong CHENG[1]

1 National Engineering Research Center of Urban Environmental Pollution Control, Beijing Municipal Research Institute of Environmental Protection, Beijing 100037, China
2 Beijing Municipal Environmental Monitoring Center, Beijing 100048, China
3 Department of Air Pollution Control, Beijing Municipal Institute of Labour Protection, Beijing 100054, China

Abstract In recent years, Beijing has experienced severe air pollution which has caused widespread public concern. Compared to the same period in 2014, the first three quarters of 2015 exhibited significantly improved air quality. However, the air quality sharply declined in the fourth quarter of 2015, especially in November and December. During that time, Beijing issued the first red alert for severe air pollution in history. In total, 2 red alerts, 3 orange alerts, 3 yellow alerts, and 3 blue alerts were issued based on the adoption of relatively temporary emergency control measures to mitigate air pollution. This study explored the reasons for these variations in air quality and assessed the effectiveness of emergency alerts in addressing severe air pollution. A synthetic analysis of emission variations and meteorological conditions was performed to better understand these extreme air pollution episodes in the fourth quarter of 2015. The results showed that compared to those in the same period in 2014, the daily average emissions of air pollutants decreased in the fourth quarter of 2015. However, the emission levels of primary pollutants were still relatively high, which was the main intrinsic cause of haze episodes, and unfavorable meteorological conditions represented important external factors. Emergency control measures for heavy air pollution were implemented during this red alert period, decreasing the emissions of primary air pollutants by approximately 36% and the $PM_{2.5}$ concentration by 11%–21%.

Keywords heavy air pollution, red alert, emissions variation, meteorological conditions, emergency control measures

Received May 11, 2017; accepted July 23, 2017

E-mails: 18701650609@163.com (Zhanshan WANG), xueyifeng@cee.cn (Yifeng XUE)

1 Introduction

Severe haze pollution events frequently occur in developing countries because of rapid industrialization and urbanization, and these events exhibit characteristics that are similar to those of previous events in developed nations (Huang et al., 2014; Lv et al., 2017). Fine particulate matter (PM), which can affect atmospheric visibility and deteriorate local and regional air quality, has become a major pollutant in northeastern China (Zhang et al., 2012; Andersson et al., 2015; Chen et al., 2015; Hsu et al., 2017). Beijing and its surrounding areas frequently experience severe haze or smog days, especially during winter. A series of pollution control policies was recently implemented in Beijing to reduce air pollutant emissions. Such policies include the Clean Air Action Plan of Beijing (2013–2017), as well as reduction and control strategies for coal-based emissions, vehicle emissions, and dust. The average $PM_{2.5}$ concentration in 2015 was 80.6 $\mu g \cdot m^{-3}$, which was 6.2% lower than that in 2014 (BJEPB, 2015a, 2016). Although the air quality of Beijing has slightly improved, the $PM_{2.5}$ concentration is still 1.3 times higher than the national standard and considerably higher than the World Health Organization (WHO) standard (Guo et al., 2013; Li et al., 2013; Chen et al., 2015; Schleicher et al., 2015; Ji et al., 2016; Park et al., 2016). Twenty-two heavy air pollution (HAP) days occurred in November and December 2015, accounting for half of the total HAP days throughout the year. This period has attracted considerable attention from the government and the public because of the effects of HAP on human health and the environment

(Djalalova et al., 2015; Yang et al., 2015; Zhou et al., 2016; Li et al., 2017). Therefore, exploring the reasons for the severe air pollution in the fourth quarter of 2015 is important.

Severe air pollution episodes often occur because of two factors: variations in emissions from regional and local pollution sources and meteorological conditions (Amil et al., 2015; Li et al., 2015; Sun et al., 2015; Tian et al., 2015). In the beginning of winter, air pollution sources considerably increase because of residential heating, and therefore emission rates of air pollutants from local pollution sources are higher during winter than in other seasons. This combination of high emissions and unfavorable meteorological conditions (stabilization of the atmospheric boundary layer, temperature inversion, etc.) can lead to severe air pollution. Several studies (Sun et al., 2006, 2014; Liu et al., 2013; Gao et al., 2015; Li et al., 2015; Zheng et al., 2015) have analyzed typical severe air pollution episodes in Beijing, including the typical months of severe pollution and the potential causes. For example, Zheng et al. (2015) used observational data and an air quality model to analyze the severe pollution in the winter of 2012−2013 in Beijing. This study also discussed the influences and contributions of meteorological conditions and variations in the regional emissions of pollutants. Cheng et al. (2015) combined numerical modeling and observational data to analyze the atmospheric background, meteorological conditions, and formation of four typical severe air pollution episodes in October 2014 in Beijing. These studies revealed the conditions associated with the formation of severe pollution, the related physical-chemical reactions and processes, and the characteristics of the variations in $PM_{2.5}$ chemical components.

However, the air pollution episodes in the fourth quarter of 2015 were unlike past episodes. In accordance with the Emergency Plan for Heavy Air Pollution in Beijing (BJEPB, 2015b), a red alert was issued because of severe pollution for the first time in history, and temporary emergency control measures were implemented. The pollution process of this episode involved the combined effects of emission variations, meteorological conditions, and the temporal control of pollution emissions. To better understand this severe pollution process, we analyzed observed air quality data and meteorological factors and explored the potential causes of HAP. Additionally, we examined the spatial and temporal evolution of HAP and evaluated the effectiveness of emergency control measures to provide a reference for pollution prevention and control during winter.

2 Materials and methods

2.1 Study area

Beijing is located at 39°56′N and 116°20′E on the northwestern edge of the North China Plain. Beijing is surrounded by the Taihang and Yanshan Mountains to the west, north, and northeast. This city covers 16,410.54 km^2, is divided into 16 districts, and is inhabited by approximately 21,148,000 residents. The demands for energy in the industrial and residential heating sectors are relatively high (Xue et al., 2016a).

2.2 Data sources

$PM_{2.5}$ concentrations in Beijing were obtained from 11 real-time monitoring sites (Fig. 1) in the Beijing Municipal Environmental Protection Monitoring Center. These meteorological data were taken from ground observations at the Beijing Municipal Observatory. The emission inventories of primary air pollutants in Beijing in 2014 and 2015 were obtained from the Beijing Municipal Research Institute of Environmental Protection. The methodology of developing the emission inventory was described in a previous study (Zhao et al., 2015). The emission reductions under yellow, orange, and red HAP alerts were calculated based on different types of pollution sources (stationary, mobile, and fugitive pollution sources).

2.3 Model configuration and simulation design

The Models-3 Community Multiscale Air Quality (CMAQ v5.0.2) (Byun and Schere, 2006; Foley et al., 2015; Syrakov et al., 2016) model with the SAPRC07 gas-phase chemical mechanism and AERO6 aerosol module was employed to simulate the pollutant concentrations. The triple-nested domains were used in the simulation, and the grid resolutions of the domains were 36 km, 12 km, and 4 km. The vertical resolution included 13 layers that extended from the surface to the tropopause, with approximately 18 m for the first layer.

The meteorological fields and emission inputs were provided by the Weather Research and Forecasting (WRF v3.6) (Syrakov et al., 2016) and Sparse Matrix Operator Kernel Emissions (SMOKE v3.5.1) (Gan et al., 2015; Wang et al., 2015a, b), respectively. The first domain used data from the multiresolution emission inventory of China (MEIC) with a 0.25° × 0.25° resolution. The two inner domains used local inventories, as discussed in section 2.2. The modeling period extended from September 26, 2015, to December 31, 2015, including model initialization from September 26 to 30, model evaluation from October 1 to November 30 and the assessment of the two red alerts in December. Two simulations were performed. Simulation 1 (SIM1) considered the emergency control measures of the two red alerts and a reduction in pollutant emissions based on the emission inventory. Simulation 2 (SIM2) did not include these factors. The difference between SIM1 and SIM2 represented the estimated effects of the emergency control measures of the red alerts.

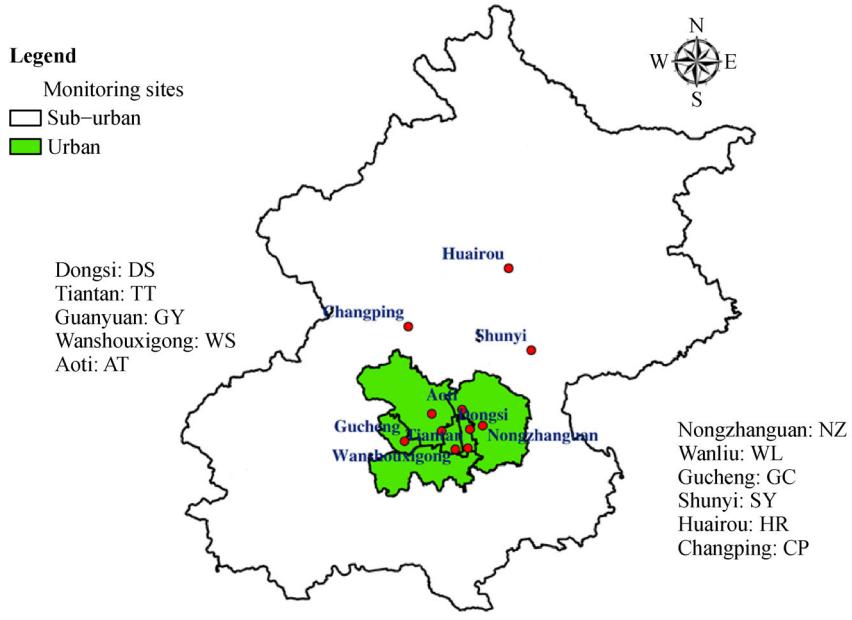

Fig. 1 Monitoring sites in this study.

2.4 Model evaluation

The simulated meteorological fields (wind speed, wind direction, temperature, and humidity) and $PM_{2.5}$ concentrations were compared to observations from October 1 to November 30 following the protocol in the literature (Emery et al., 2001; Wang et al., 2010).

Table 1 presents the performance of the WRF model for the simulated meteorological variables. All four statistics (mean bias (MB), mean absolute gross error (MAGE), root mean square error (RMSE), and index of agreement (IOA)) were within the typical ranges for meteorological modeling studies (Emery et al., 2001; Wang et al., 2010).

Table 1 Performance of the WRF-simulated meteorological fields

Variable	MB	MAGE	RMSE	IOA
Temperature	0.51 K	1.15 K	-	0.79
Humidity	−2.50 g/kg	1.50 g/kg	-	0.68
Wind speed	0.22 m/s	-	0.39 m/s	0.81
Wind direction	2.66 deg	20.61 deg	-	-

Figure 2 compares the simulated and observed daily average concentrations of $PM_{2.5}$ in Beijing. CMAQ reasonably reproduced the temporal variations, with a correlation coefficient of 0.82. Compared to the observations, CMAQ slightly overestimated the $PM_{2.5}$ concentrations. The normalized mean bias and normalized mean error values were 0.05 and 0.35, respectively, which may be due to the uncertainty in the emission inventory and inaccuracy of the simulated meteorological fields. Generally, the model performance was comparable to the performance reported in previous studies (Simon et al., 2012; Gan et al., 2015; Hogrefe et al., 2015; Wang et al., 2015b) and is adequate for our study.

3 Results and discussion

3.1 Emission variations

The emission variations were calculated based on the air pollutant emission inventory of Beijing in 2014 and 2015. The considered source categories included fuel combustion, industrial production processes, mobile sources, solvent use, agricultural practices, fugitive dust, biomass burning, waste processing, the storage and transport of oil and gas, and others (BMRIEP, 2016). A detailed description of the calculations can be found in the literature (Zhao et al., 2015). Figure 3 compares the emission variations with and without emergency control measures in the fourth quarter of 2014 and 2015. Without the temporary control measures during the 21st Asia-Pacific Economic Cooperation (APEC) period (November 3 to 12) in 2014 and the red, orange, and yellow alerts for HAP, the daily average emissions of SO_2, NO_x, PM_{10}, $PM_{2.5}$ and VOCs in the fourth quarter of 2015 were 7.3%, 7.6%, 0.1%, 2.1%, and 5.4% less than those during the same period in 2014. The main reason for these reductions was the implementation of normal control measures in 2015 according to the Clean Air Action Plan. These measures included the elimination of 3,800,000 old vehicles; the closure of two coal-fired power plants (Guohua and Gaojing) and two cement plants

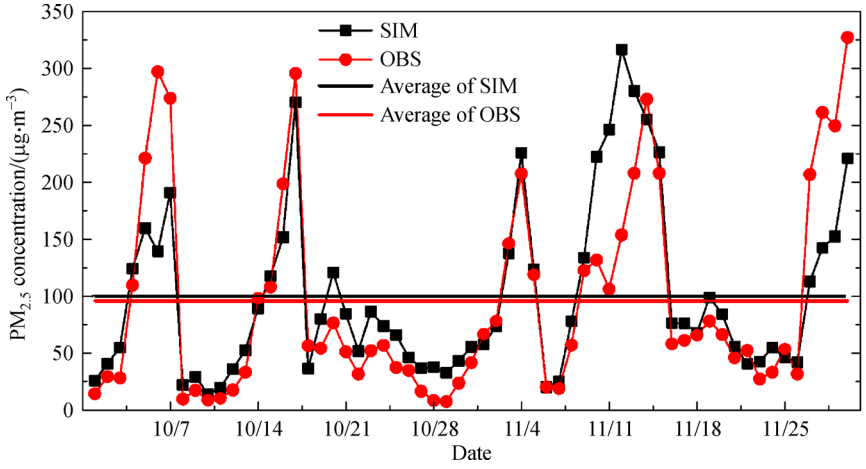

Fig. 2 Comparison of simulated (SIM) and observed (OBS) daily average concentrations of $PM_{2.5}$ in Beijing.

(Xiafa and Qianglian); the conversion of coal-fired industrial boilers with capacities greater than 6000 t/h to gas-fired boilers; the advancement of environmental technology; and the improved treatment of VOCs emitted from chemical, car manufacturing, furniture, painting, and other industries. However, the decline in PM was not significant because of a lack of effective control measures for fugitive dust, which was the major source of PM.

Beijing initially adopted temporary emergency control measures to improve the air quality during haze periods. From November 3 to 12, 2014, the use of private vehicles was restricted based on even- and odd-numbered license plates, which effectively prohibited millions of registered cars from driving on the streets and improved the air quality during the APEC period. In addition, operations at hundreds of manufacturing factories were suspended during that period. From November to December 2015, 2 red, 3 orange, 3 yellow, and 3 blue alerts were issued for HAP. The emergency control measures that were implemented during this time included vehicle controls, industrial production limits, construction stoppages, and other measures. In contrast, 0 red, orange, and yellow alerts and only 3 blue alerts were issued for HAP during the same period in 2014. After implementing these emergency control measures, the daily average emissions of SO_2, NO_x, PM_{10}, $PM_{2.5}$, and VOCs during the fourth quarter of 2015 were 5.6%, 7.6%, 2.0%, 3.1%, and 5.3% lower than those during the same period in 2014 (Xue et al., 2016b). Thus, the emissions of these major air pollutants were reduced by an average of 4.7%.

Furthermore, a large difference existed in monthly emissions; the emission reduction in October was particularly large. Compared to those in the 2014 period, the daily average emissions of SO_2 decreased by 17.8% because of the implementation of pollution controls and energy structure adjustments. In November 2015, the daily average emissions of SO_2, NO_x, PM_{10}, $PM_{2.5}$, and VOCs increased by 5.1%, 3.1%, 17.7%, 13.2%, and 3.9%, respectively, compared to those during the same period in 2014. The main reason for these increases was the influence of temporary control measures during the APEC period. Because of the poor air quality in December 2015, Beijing issued its first ever red alert for severe air pollution, adopted strict emergency control measures, and enhanced the enforcement and supervision of pollution sources. Although air pollutants still accumulated in the atmosphere, the absolute emissions of primary air pollutants were controlled. The emissions of primary air pollutants were reduced by an average of 14% compared to the average in 2014. In 2015, the emission reduction rate of the HAP emergency control measures was higher than that during the APEC period, but the corresponding air quality did not improve. The results suggest that adverse weather conditions dominated the pollution process during the fourth quarter of 2015.

3.2 Meteorological conditions

Unfavorable meteorological conditions were one of the main factors that led to HAP (Porter et al., 2015; Zhang et al., 2015; Bei et al., 2016). Figure 4 presents the meteorological conditions from October to December 2015 and those during the same period in 2014. The average temperature and relative humidity during these three months in 2015 were 6.5°C and 65.3%, which were 10.2% and 25.6% higher than those during the same period in 2014, respectively. The average ground-level pressure and wind speed during these three months in 2015 were 1020 hPa and 1.9 $m \cdot s^{-1}$, which were 2.9 hPa and 29.6% lower than those during the same period in 2014, respectively. Overall, the average temperature and relative humidity in 2015 were higher than those in 2014, whereas the ground-level pressure and wind speed in 2015 were lower than those in 2014. High humidity conditions promote the hygroscopic growth of particulates, which subsequently increases the mass concentration of

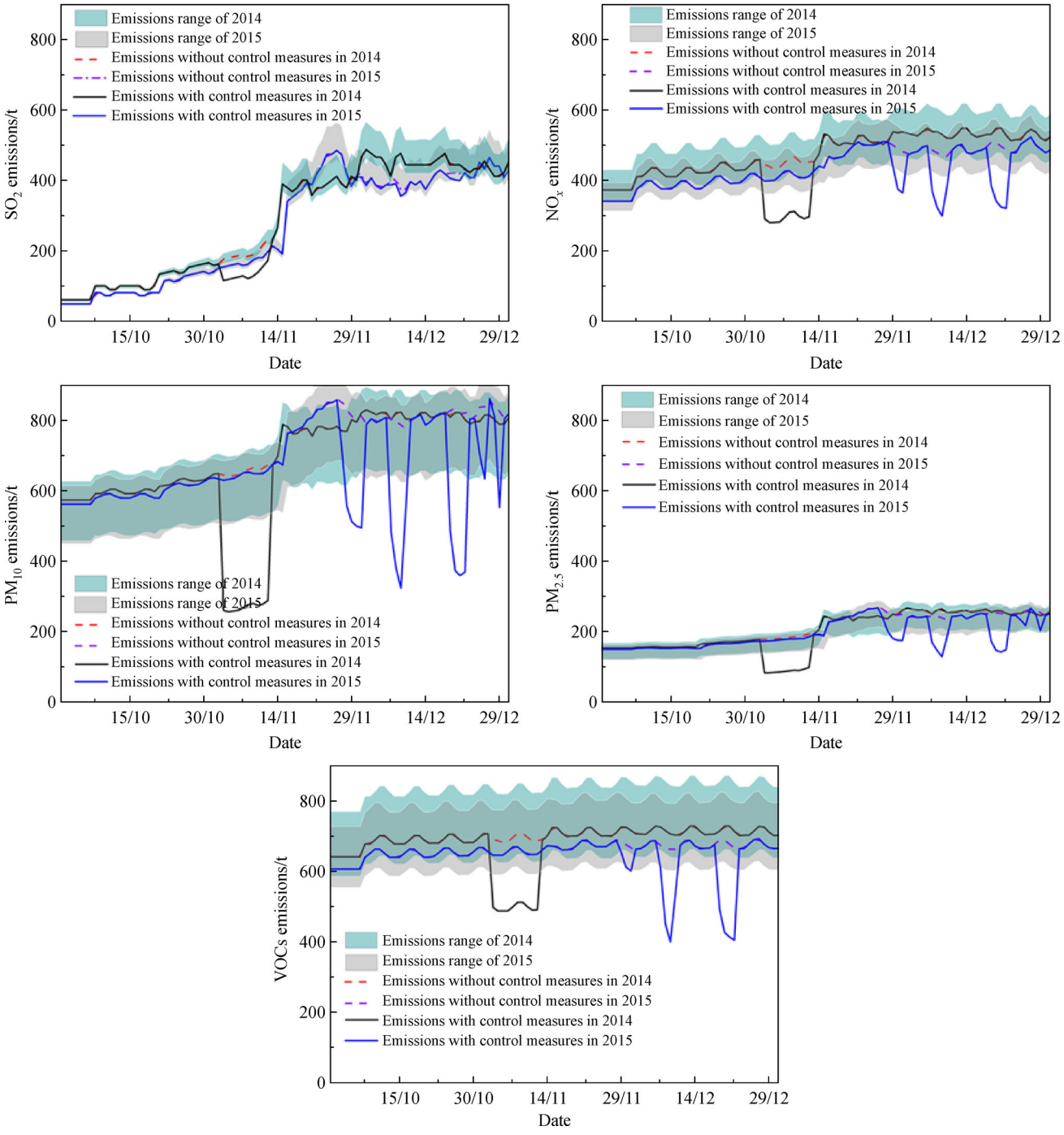

Fig. 3 Comparison of variations in air pollutant emission from October to December of 2014 and 2015 in Beijing.

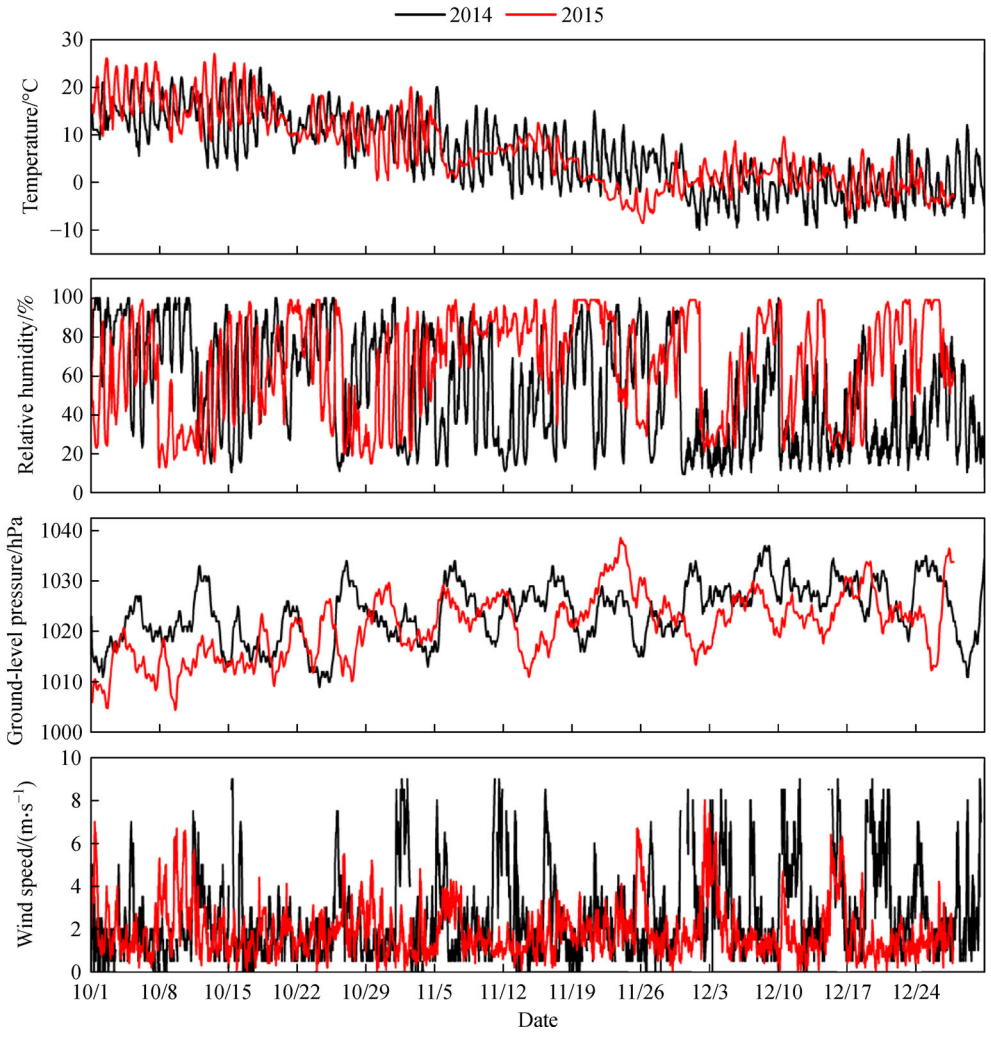

Fig. 4 Meteorological conditions from October to December of 2014 and 2015.

pollutants and causes severe haze episodes. In addition, wind speed is negatively correlated with the $PM_{2.5}$ concentration (Hsu et al., 2017). Thus, compared to those in the same period in 2014, the meteorological conditions in 2015 were unfavorable for the dispersal of air pollutants.

3.3 Air quality in Beijing during the fourth quarter of 2015

The concentration of $PM_{2.5}$ in Beijing during the fourth quarter (October, November, and December) of 2015 ranged from 74.5–152.0 $\mu g \cdot m^{-3}$, with an average concentration of 114.8 $\mu g \cdot m^{-3}$. According to the Air Quality Index (AQI) standard (HJ 633-2012), HAP days refer to daily average concentrations of $PM_{2.5}$ that exceed 150 $\mu g \cdot m^{-3}$. During October, November, and December, 27 HAP days were observed, accounting for 29.3% of the three months (Table 2 and Fig. 5). The highest daily average $PM_{2.5}$ concentration was 477.1 $\mu g \cdot m^{-3}$, which occurred on December 1. The longest continuous HAP event occurred from November 27 to December 1 (5 days), and the average concentration of $PM_{2.5}$ was 307.0 $\mu g \cdot m^{-3}$ during this episode.

Figure 6 illustrates the average cumulative $PM_{2.5}$ concentrations (average concentrations of $PM_{2.5}$ from October 1 to December 31) and their variations in 2014 and 2015. After implementing temporary control measures to improve the air quality during the APEC period, the average monthly $PM_{2.5}$ concentration in November 2014 was lower than that during the same period in 2015. Implementing the conventional control measures from the Clean Air Action Plan in 2015 decreased the average concentration in October 2015 by 37.1% compared to that during the same period in 2014, as shown in Fig. 5. Because of the high $PM_{2.5}$ concentration in October 2014, the air quality improvement in November 2014 was largely offset. Therefore, the cumulative concentrations from October to November were higher in 2014 than in 2015. The average cumulative concentration of $PM_{2.5}$ in December 2015 exceeded that in December 2014, as did

Table 2 Days of different air quality grades from October to December 2015

Month	Air quality grades (concentration range/μg·m^{-3})					
	Grade I (0–35)	Grade II (35–75)	Grade III (75–115)	Grade IV (115–150)	Grade V (150–250)	Grade VI (>250)
October	15	8	3	0	2	3
November	4	10	4	3	5	4
December	5	6	3	4	7	6

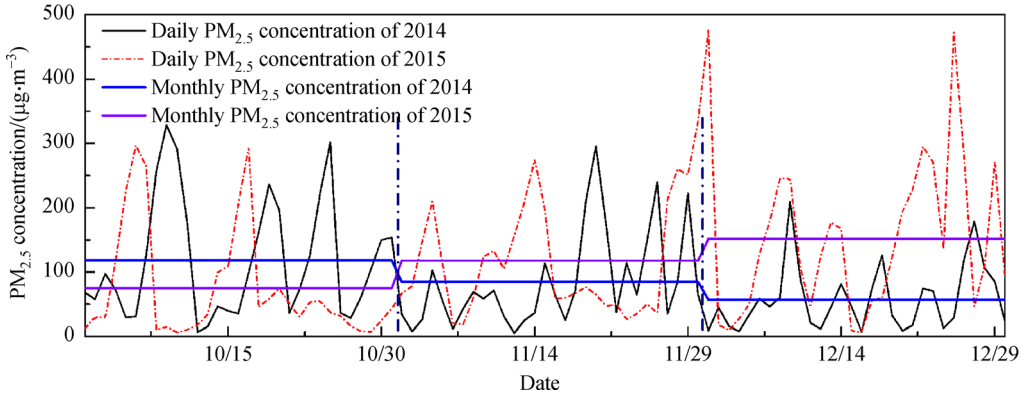

Fig. 5 Daily average concentrations of $PM_{2.5}$ at national control sites in Beijing during the fourth quarter of 2015.

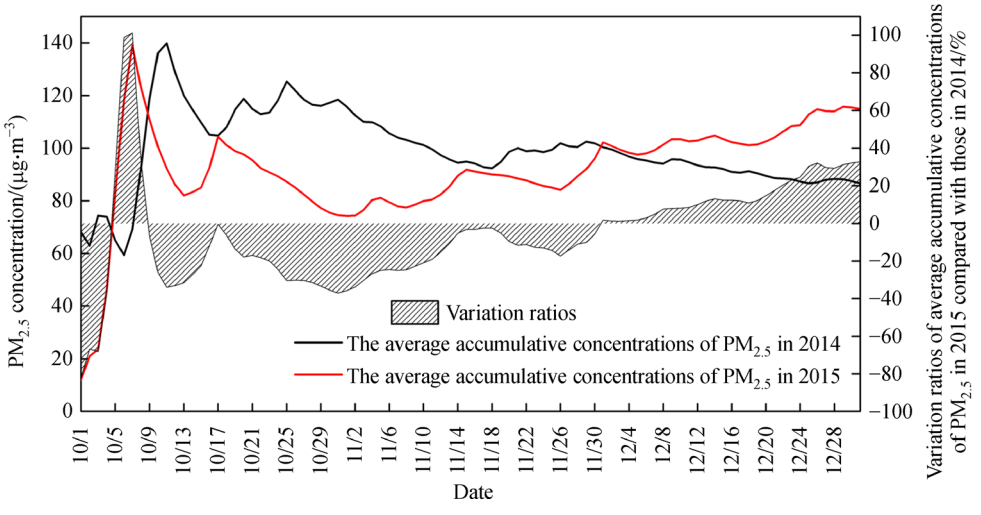

Fig. 6 Average cumulative $PM_{2.5}$ concentrations and their variations in 2014 and 2015.

the concentrations during several HAP episodes. At the end of the fourth quarter in 2015, the average cumulative concentration of $PM_{2.5}$ was 32.6% higher than that in 2014.

As shown in Fig. 7, the average concentrations of $PM_{2.5}$ on HAP days (242.6 μg·m^{-3}) were significantly higher (4.6 times) than those on other days (NHAP days, 52.8 μg·m^{-3}) in Beijing. The highest concentration difference was 215.5 μg·m^{-3}, which occurred at the WS site. The lowest concentration difference was 146.1 μg·m^{-3}, which occurred at the CP site. The average concentration difference was 189.8 μg·m^{-3} during the three months, and the concentration differences in the northern region of Beijing were lower than those in urban Beijing, indicating that the influence of HAP was more obvious at urban sites.

Figure 8 shows the spatial distribution of $PM_{2.5}$ on HAP days and NHAP days based on the kriging method. On both HAP days and NHAP days, the $PM_{2.5}$ concentrations in the southern region of Beijing were higher than those in the northern region. On NHAP days, the average $PM_{2.5}$ concentrations were lower than 40 μg·m^{-3} in the northern

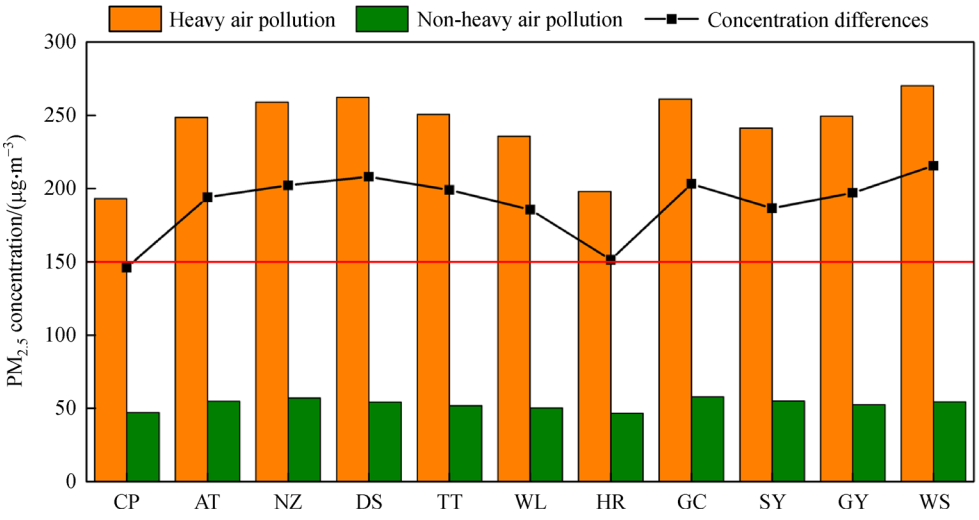

Fig. 7 Average concentrations of $PM_{2.5}$ on HAP days and NHAP days during the fourth quarter of 2015.

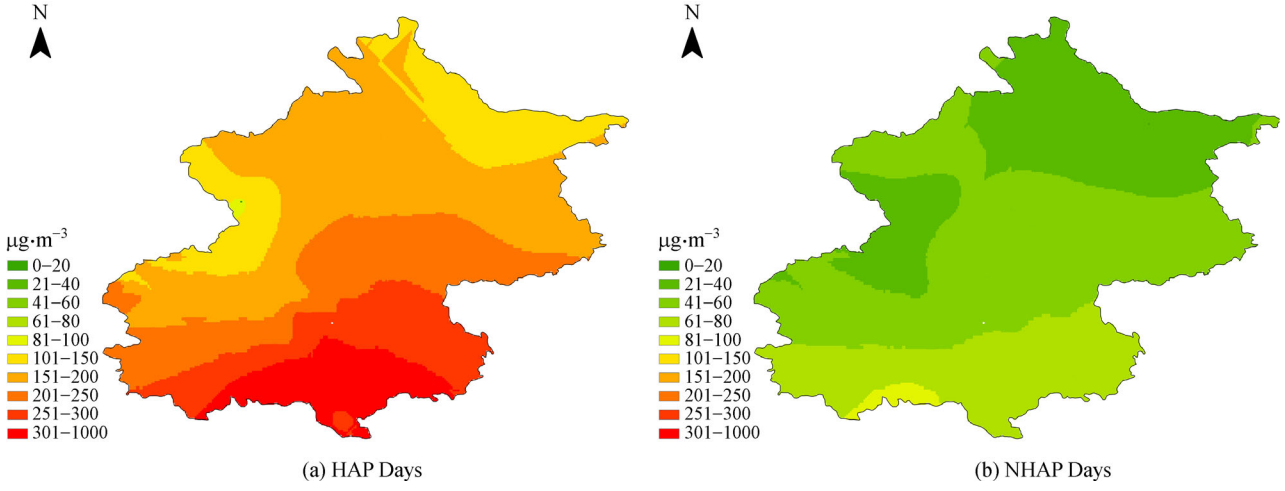

Fig. 8 Spatial distribution of $PM_{2.5}$ concentrations on HAP days (a) and NHAP days (b) during the fourth quarter of 2015.

mountainous region of Beijing and lower than 60 $\mu g \cdot m^{-3}$ in urban Beijing. The $PM_{2.5}$ concentrations ranged from 80−100 $\mu g \cdot m^{-3}$ and were highest in the southwestern region of Beijing. On HAP days, the average $PM_{2.5}$ concentrations were higher than 300 $\mu g \cdot m^{-3}$ and 250 $\mu g \cdot m^{-3}$ in the southern and urban regions of Beijing, respectively. The $PM_{2.5}$ concentrations exceeded 150 $\mu g \cdot m^{-3}$ in most of the northern regions. Thus, all of Beijing experienced serious air pollution on HAP days.

3.4 Assessment of the two HAP red alerts in December 2015

Beijing issued an orange alert for HAP at 00:00 a.m. on December 7, which was upgraded to a red alert at 7:00 a.m. on December 8. At 12:00 p.m. on December 10, the red alert was dismissed. The simulation results in Fig. 9 show that the $PM_{2.5}$ concentration decreased by an average of 16.1%. The implementation of the red alert decreased the magnitude of the peak concentration and decelerated the pollution growth. On December 8, the $PM_{2.5}$ concentration significantly decreased by 16.8% after the red alert was issued. On December 9, the diffusion conditions were still unfavorable; combined with the southward pollution transport, the $PM_{2.5}$ concentrations should have continuously increased. However, the $PM_{2.5}$ growth slowed because of the implementation of emergency control measures, decreasing the $PM_{2.5}$ concentration to the same level as that on December 8.

The $PM_{2.5}$ concentration on December 9 was 16.7% lower than that without any emergency control measures after the alert was issued (SIM2). On December 10, the $PM_{2.5}$ concentration decreased with improved meteorological conditions and emergency control measures (SIM1).

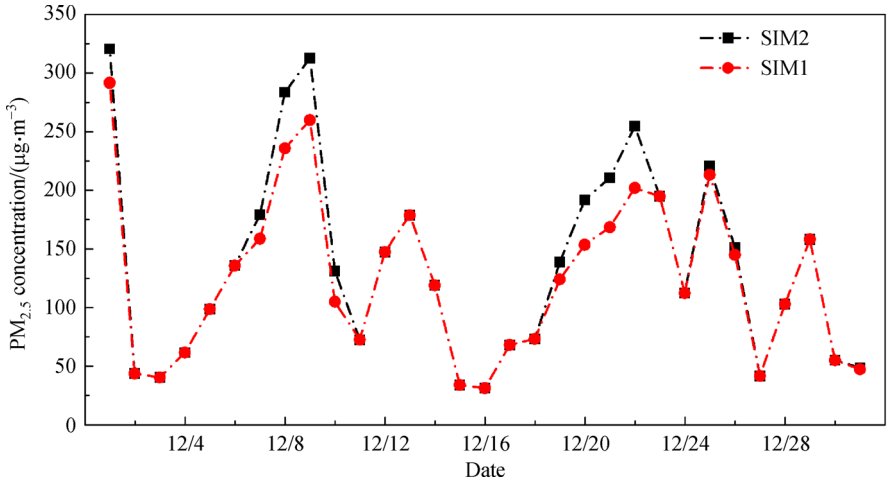

Fig. 9 Variations in the $PM_{2.5}$ concentrations with and without the emergency control measures that were implemented during the two red alerts.

The emergency control measures resulted in a 20.1% decrease in the $PM_{2.5}$ concentration. Spatially, the decrease in the $PM_{2.5}$ concentration, which was approximately 10%, was most obvious in the six major urban districts, Daxing, Tongzhou, and eastern Fangshan (Fig. 10).

Beijing issued another red alert for severe air pollution at 7:00 a.m. on December 19, which was dismissed at 00:00 a.m. on December 22. Figure 11 shows that the air quality

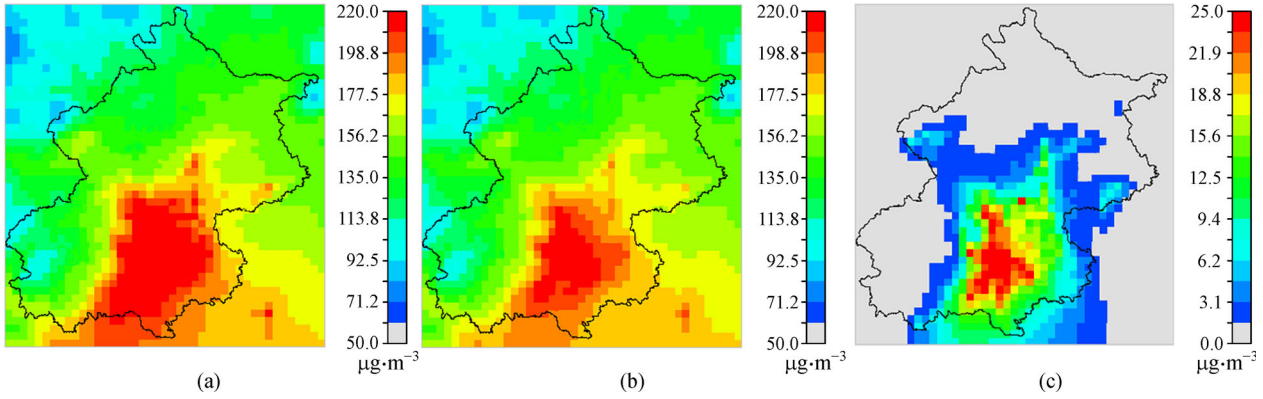

Fig. 10 Spatial distribution of the $PM_{2.5}$ concentration averaged from December 7 to 10 in SIM2 (a) and SIM1 (b), as well as the difference between SIM2 and SIM1 (c).

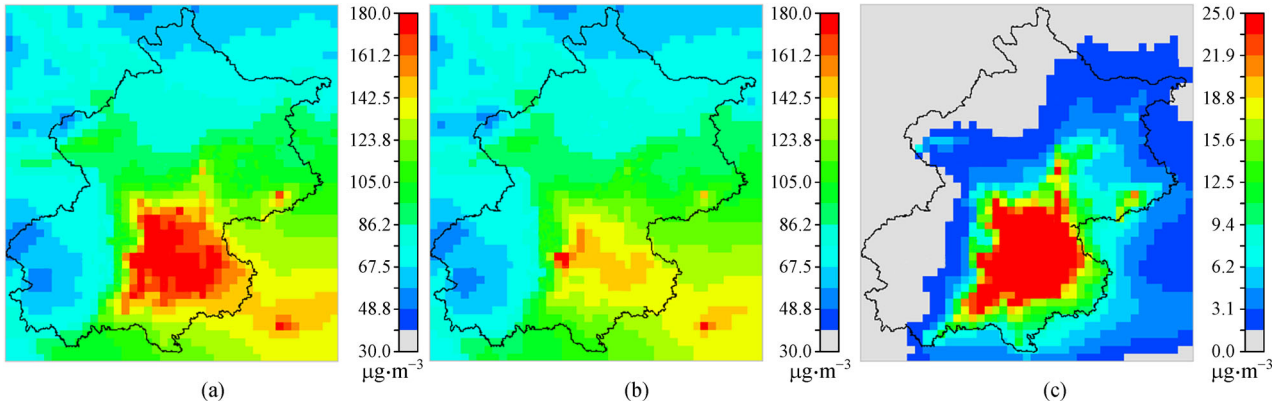

Fig. 11 Spatial distribution of the $PM_{2.5}$ concentration averaged from December 19 to 22 in SIM2 (a) and SIM1 (b), as well as the difference between SIM2 and SIM1 (c).

improved after emergency control measures were adopted, and the $PM_{2.5}$ concentration decreased by an average of 17.9%. On December 19, the $PM_{2.5}$ concentration decreased by 10.6% after the red alert was issued. From December 20 to 22, the diffusion conditions worsened and the $PM_{2.5}$ concentration increased, leading to more serious pollution. The $PM_{2.5}$ concentration decreased by at least 50 $\mu g \cdot m^{-3}$ each day. Although these red alert measures were unable to alleviate the pollution, they still slowed the increase in the $PM_{2.5}$ concentration. Significant decreases in the $PM_{2.5}$ concentration occurred, mainly in the six major urban districts and surrounding areas.

4 Conclusions

This study explored the reasons for the severe air pollution that occurred in the fourth quarter of 2015 by comparing the emissions from air pollution sources, meteorological conditions and the ambient $PM_{2.5}$ variance in the fourth quarter of 2015 and that in 2014. Model simulations were used to assess the environmental effects of the emergency control measures for severe air pollution. The results were as follows:

1) Compared to those during the same period in 2014, the major air pollutant emissions were smaller in the fourth quarter of 2015 due to the implementation of control measures based on the Beijing Clean Air Action Plan. However, the air pollutant emissions still exceeded the environmental capacity due to the demand for heating during winter. High consumption levels of coal and natural gas were the main factors for the severe air pollution that occurred in November and December 2015.

2) The meteorological conditions were the key external factors that affected air pollution. A low ground wind speed, stable atmospheric boundary layer, high relative humidity, and low planetary boundary layer height caused poor horizontal and vertical diffusion, which intensified air pollution.

3) The emergency control measures that were implemented during the red alert decreased pollutant emissions by approximately 36% and the $PM_{2.5}$ concentration by 11%−21%. The meteorological conditions during this severe air pollution period caused air pollutant accumulation and secondary reactions. The greatest effect of the emergency control measures for pollution emission reduction occurred 48−72 h after the alert was issued. Thus, the optimum issue time for control measures is 36−48 h before the rapid increase in the $PM_{2.5}$ concentration. Implementing measures during this period should help to prevent severe $PM_{2.5}$ pollution. Thus, air quality alerts should be based on accurate pollution forecasts.

Acknowledgements This work was funded by the National Science and Technology Support Program of the Ministry of Science and Technology of China (Nos. 2014BAC23B02, 2014BAC23B03 and 2014BAC06B05), the Science Foundation of Beijing Municipal Research Institute of Environmental Protection (No. 2014A04), and the Beijing Excellent Personnel Training Project (No. 2015000021733G173). The authors also thank the MEIC team from Tsinghua University for providing the 36-km emission inventory.

References

Amil N, Latif M T, Khan M F, Mohamad M (2015). Meteorological-gaseous influences on seasonal $PM_{2.5}$ variability in the Klang valley urban-industrial environment. Atmos Chem Phys Discuss, 15(18): 26423–26479

Andersson A, Deng J, Du K, Zheng M, Yan C, Sköld M, Gustafsson Ö (2015). Regionally-varying combustion sources of the January 2013 severe haze events over eastern China. Environ Sci Technol, 49(4): 2038–2043

Bei N, Xiao B, Meng N, Feng T (2016). Critical role of meteorological conditions in a persistent haze episode in the Guanzhong basin, China. Sci Total Environ, 550: 273–284

BJEPB (Beijing Municipal Environmental Protection Bureau) (2015a). Beijing Environmental Statement 2014

BJEPB (Beijing Municipal Environmental Protection Bureau) (2015b). Emergency plan for heavy air pollution in Beijing

BJEPB (Beijing Municipal Environmental Protection Bureau) (2016). Beijing Environmental Statement 2015

BMRIEP (Beijing Municipal Research Institute of Environmental Protection) (2016). Technical Report for Emission Inventory of Primary Air Pollutants in Beijing, 2015

Byun D, Schere K L (2006). Review of the governing equations, computational algorithms, and other components of the models-3 Community Multiscale Air Quality (CMAQ) modeling system. Appl Mech Rev, 59(2): 51–77

Chen W, Yan L, Zhao H (2015). Seasonal variations of atmospheric pollution and air quality in Beijing. Atmosphere, 6(12): 1753–1770

Cheng N, Li Y, Zhang D, Chen T, Xu W, Sun F, Dong X (2015). Analysis about the characteristics and formation mechanisms of a serious pollution event in October 2014 in Beijing. Research of Environmental Sciences, 28: 163–170

Djalalova I, Delle Monache L, Wilczak J (2015). $PM_{2.5}$ analog forecast and Kalman filter post-processing for the Community Multiscale Air Quality (CMAQ) model. Atmos Environ, 108: 76–87

Emery C, Tai E, Yarwood G (2001). Enhanced meteorological modeling and performance evaluation for two Texas ozone episodes. Prepared for The Texas Natural Resource Conservation Commission by ENVIRON International Corporation. 2001

Foley K M, Hogrefe C, Pouliot G, Possiel N, Roselle S J, Simon H, Timin B (2015). Dynamic evaluation of CMAQ Part I: separating the effects of changing emissions and changing meteorology on ozone levels between 2002 and 2005 in the eastern US. Atmospheric Environment 103: 247–255

Gan C M, Binkowski F, Pleim J, Xing J, Wong D, Mathur R, Gilliam R (2015). Assessment of the aerosol optics component of the coupled WRF–CMAQ model using CARES field campaign data and a single column model. Atmos Environ, 115: 670–682

Gao J, Tian H, Cheng K, Lu L, Zheng M, Wang S, Hao J, Wang K, Hua

S, Zhu C, Wang Y (2015). The variation of chemical characteristics of $PM_{2.5}$ and PM_{10} and formation causes during two haze pollution events in urban Beijing, China. Atmos Environ, 107: 1–8

Guo S, Hu M, Guo Q, Zhang X, Schauer J J, Zhang R (2013). Quantitative evaluation of emission controls on primary and secondary organic aerosol sources during Beijing 2008 Olympics. Atmos Chem Phys, 13(16): 8303–8314

Hogrefe C, Pouliot G, Wong D, Torian A, Roselle S, Pleim J, Mathur R (2015). Annual application and evaluation of the online coupled WRF–CMAQ system over North America under AQMEII phase 2. Atmos Environ, 115: 683–694

Hsu C Y, Chiang H C, Chen M J, Chuang C Y, Tsen C M, Fang G C, Tsai Y I, Chen N T, Lin T Y, Lin S L, Chen Y C (2017). Ambient $PM_{2.5}$ in the residential area near industrial complexes: spatiotemporal variation, source apportionment, and health impact. Sci Total Environ, 590–591: 204–214

Huang R J, Zhang Y, Bozzetti C, Ho K F, Cao J J, Han Y, Daellenbach K R, Slowik J G, Platt S M, Canonaco F, Zotter P, Wolf R, Pieber S M, Bruns E A, Crippa M, Ciarelli G, Piazzalunga A, Schwikowski M, Abbaszade G, Schnelle-Kreis J, Zimmermann R, An Z, Szidat S, Baltensperger U, El Haddad I E, Prévôt A S H (2014). High secondary aerosol contribution to particulate pollution during haze events in China. Nature, 514(7521): 218–222

Ji D, Zhang J, He J, Wang X, Pang B, Liu Z, Wang L, Wang Y (2016). Characteristics of atmospheric organic and elemental carbon aerosols in urban Beijing, China. Atmos Environ, 125: 293–306

Li J, Du H Y, Wang Z F, Sun Y L, Yang W Y, Li J J, Tang X, Fu P F (2017). Rapid formation of a severe regional winter haze episode over a mega-city cluster on the North China Plain. Environ Pollut, 223: 605–615

Li J, Xie S D, Zeng L M, Li L Y, Li Y Q, Wu R R (2015). Characterization of ambient volatile organic compounds and their sources in Beijing, before, during, and after Asia-Pacific Economic cooperation China 2014. Atmos Chem Phys, 15(14): 7945–7959

Li Z, Gu X, Wang L, Li D, Xie Y, Li K, Dubovik O, Schuster G, Goloub P, Zhang Y, Li L, Ma Y, Xu H (2013). Aerosol physical and chemical properties retrieved from ground-based remote sensing measurements during heavy haze days in Beijing winter. Atmos Chem Phys, 13(20): 10171–10183

Liu X G, Li J, Qu Y, Han T, Hou L, Gu J, Chen C, Yang Y, Liu X, Yang T, Zhang Y, Tian H Z, Hu M (2013). Formation and evolution mechanism of regional haze: a case study in the megacity Beijing, China. Atmos Chem Phys, 13(9): 4501–4514

Lv B, Cai J, Xu B, Bai Y Q (2017). Understanding the rising phase of the $PM_{2.5}$ concentration evolution in Large China cities. Sci Rep, 7: 46456

Park S U, Lee I H, Joo S J (2016). Spatial and temporal distributions of aerosol concentrations and depositions in Asia during the year 2010. Science of the Total Environment, 542(A): 210–222

Porter W C, Heald C L, Cooley D, Russell B (2015). Investigating the observed sensitivities of air-quality extremes to meteorological drivers via quantile regression. Atmos Chem Phys, 15(18): 10349–10366

Schleicher N J, Schäfer J, Blanc G, Chen Y, Chai F, Cen K, Norra S (2015). Atmospheric particulate mercury in the megacity Beijing: spatio-temporal variations and source apportionment. Atmos Environ, 109: 251–261

Simon H, Baker K R, Phillips S (2012). Compilation and interpretation of photochemical model performance statistics published between 2006 and 2012. Atmos Environ, 61: 124–139

Sun Y, Du W, Wang Q, Zhang Q, Chen C, Chen Y, Chen Z, Fu P, Wang Z, Gao Z, Worsnop D R (2015). Real-time characterization of aerosol particle composition above the urban canopy in Beijing: insights into the interactions between the atmospheric boundary layer and aerosol chemistry. Environ Sci Technol, 49(19): 11340–11347

Sun Y, Jiang Q, Wang Z, Fu P, Li J, Yang T, Yin Y (2014). Investigation of the sources and evolution processes of severe haze pollution in Beijing in January 2013. J Geophys Res D Atmospheres, 119(7): 4380–4398

Sun Y, Zhuang G, Tang A A, Wang Y, An Z (2006). Chemical characteristics of $PM_{2.5}$ and PM_{10} in haze-fog episodes in Beijing. Environ Sci Technol, 40(10): 3148–3155

Syrakov D, Prodanova M, Georgieva E, Etropolska I, Slavov K (2016). Simulation of European air quality by WRF–CMAQ models using AQMEII-2 infrastructure. J Comput Appl Math, 293: 232–245

Tian H Z, Zhu C Y, Gao J J, Cheng K, Hao J M, Wang K, Hua S B, Wang Y, Zhou J R (2015). Quantitative assessment of atmospheric emissions of toxic heavy metals from anthropogenic sources in China: historical trend, spatial distribution, uncertainties, and control policies. Atmos Chem Phys, 15(17): 10127–10147

Wang L, Wei Z, Wei W, Fu J S, Meng C, Ma S (2015a). Source apportionment of $PM_{2.5}$ in top polluted cities in Hebei, China using the CMAQ model. Atmos Environ, 122: 723–736

Wang N, Guo H, Jiang F, Ling Z H, Wang T (2015b). Simulation of ozone formation at different elevations in mountainous area of Hong Kong using WRF-CMAQ model. Sci Total Environ, 505: 939–951

Wang X, Zhang Y, Hu Y, Zhou W, Lu K, Zhong L, Zeng L, Shao M, Hu M, Russell A G (2010). Process analysis and sensitivity study of regional ozone formation over the Pearl River Delta, China, during the PRIDE-PRD2004 campaign using the community multiscale air quality modeling system. Atmos Chem Phys, 10(9): 4423–4437

Xue Y, Tian H, Yan J, Zhou Z, Wang J, Nie L, Pan T, Zhou J, Hua S, Wang Y, Wu X (2016a). Temporal trends and spatial variation characteristics of primary air pollutants emissions from coal-fired industrial boilers in Beijing, China. Environ Pollut, 213: 717–726

Xue Y F, Zhou Z, Nie T, Pan T, Qi J, Nie L, Wang Z S, Li Y T, Li X F, Tian H Z (2016b). Exploring the severe haze in Beijing during December, 2015: pollution process and emissions variation. Environmental Science, 37(5): 1593–1601

Yang Y, Zhou R, Wu J, Yu Y, Ma Z, Zhang L, Di Y A (2015). Seasonal variations and size distributions of water-soluble ions in atmospheric aerosols in Beijing, 2012. J Environ Sci (China), 34: 197–205

Zhang W, Capps S L, Hu Y, Nenes A, Napelenok S L, Russell A G (2012). Development of the high-order decoupled direct method in three dimensions for particulate matter: enabling advanced sensitivity analysis in air quality models. Geosci Model Dev, 5(2): 355–368

Zhang X Y, Wang J Z, Wang Y Q, Liu H L, Sun J Y, Zhang Y M (2015). Changes in chemical components of aerosol particles in different haze regions in China from 2006 to 2013 and contribution of meteorological factors. Atmos Chem Phys, 15(22): 12935–12952

Zhao Y, Qiu L P, Xu R Y, Xie F J, Zhang Q, Yu Y Y, Nielsen C P, Qin H X, Wang H K, Wu X C, Li W Q, Zhang J (2015). Advantages of a

city-scale emission inventory for urban air quality research and policy: the case of Nanjing, a typical industrial city in the Yangtze River Delta, China. Atmos Chem Phys, 15(21): 12623–12644

Zheng G J, Duan F K, Su H, Ma Y L, Cheng Y, Zheng B, Zhang Q, Huang T, Kimoto T, Chang D, Pöschl U, Cheng Y F, He K B (2015). Exploring the severe winter haze in Beijing: the impact of synoptic weather, regional transport and heterogeneous reactions. Atmos Chem Phys, 15(6): 2969–2983

Zhou M, Wang H, Zhu J, Chen W, Wang L, Liu S, Li Y, Wang L, Liu Y, Yin P, Liu J, Yu S, Tan F, Barber R M, Coates M M, Dicker D, Fraser M, González-Medina D, Hamavid H, Hao Y, Hu G, Jiang G, Kan H, Lopez A D, Phillips M R, She J, Vos T, Wan X, Xu G, Yan L L, Yu C, Zhao Y, Zheng Y, Zou X, Naghavi M, Wang Y, Murray C J, Yang G, Liang X (2016). Cause-specific mortality for 240 causes in China during 1990−2013: a systematic subnational analysis for the Global Burden of Disease Study 2013. Lancet, 387(10015): 251–272